Construction of Wavelength/Time Codes for Fiber-Optic CDMA Networks

E. S. Shivaleela and T. Srinivas, *Member, IEEE*

***Abstract*—Fiber-optic code-division multiple-access (FO-CDMA) technology for high-speed access networks has attracted a lot of attention recently. Constructions of 2-D codes, suitable for incoherent wavelength/time (W/T) FO-CDMA, have been proposed to reduce the time spread of the 1-D sequences. The W/T construction of codes can be broadly classified as 1) hybrid sequences and 2) matrix codes. Earlier, we reported a new family of unipolar wavelength/time multiple-pulses-per-row (W/T MPR) matrix codes that have good cardinality, spectral efficiency and at the same time have the lowest off-peak autocorrelation and cross-correlation values equal to unity. In this paper, we propose an algorithm to construct W/T MPR codes, starting with distinct 1-D optical orthogonal codes (OOCs) of a family as the row vectors of the code. The 2-D optical orthogonal signature pattern codes (OOSPCs), which are also constructed from 1-D OOCs, need much higher temporal length than that of W/T MPR codes, to construct codes of given cardinality and weight. Representation of the results of the codes generated using the algorithm are presented and the correlation properties are verified. We have analyzed the performance of the W/T MPR codes considering multiple access interference as the main source of noise. Also, we have compared cardinality and spectral efficiency of the codes with other W/T codes.**

***Index Terms*—Fiber-optics (FO) communication, incoherent optical communications, optical code-division multiple access (CDMA), wavelength/time codes.**

I. Introduction

To MEET the growing demands of the high data-rate applications, suitable asynchronous multiplexing schemes such as fiber-optic code-division multiple access (FO-CDMA) with optical encoding and decoding are required. Shah has reported in [1] that the FO-CDMA offers potential benefits, but, at the same time, faces challenges in the following three areas:

1) coding algorithm and schemes;
2) advanced encoding and decoding hardware;
3) network architecture, simulation, and applications.

To mitigate the nonlinear effects in large-spread sequences of 1-D unipolar codes in FO-CDMA networks, 2-D codes [2]–[10], [16], [17] have been proposed and wavelength time (W/T) encoding of the 2-D codes is practical in FO-CDMA networks [11], [12]. W/T codes reported so far can be classified mainly into two types:

1) hybrid sequences [2], [3], [16], where one type of sequence is crossed with another to improve the cardinality and/or correlation properties;
2) conversion of 1-D sequences to 2-D codes [4]–[6] and construction [7]–[10] to reduce the "time" like property.

As a solution to the first challenge, we proposed a new family of matrix codes in [10], for incoherent FO-CDMA networks that have good cardinality, spectral efficiency, and minimal cross-correlation values. We reported the basic design principles of the new family of wavelength/time multiple-pulses-per-row (W/T MPR) codes that are characterized by $N(R\times L_T,\ W,\ \lambda_a=1,\ \lambda_c=1)$ where, N is the number of codes, R is the number of rows, L_T is the number of columns, W is the weight of the code, $W_p = W/R$ is the weight per row, λ_a is the peak out-of-phase autocorrelation, and λ_c is the peak cross correlation. The rows of a W/T MPR code are encoded by distinct wavelengths and the columns in time. A family of W/T MPR codes is assumed to have equal W_p in all the rows. This assumption is made due to the fact that unequal W_p results in unequal optical powers in the arms of the matched filter of the decoder, as the splitting ratios will vary depending on the value of W_p. A smaller W_p results in large power/arm of a decoder than that of a larger W_p, for a given optical power/chip. As a result, threshold Th values required to be set at various receivers will vary and result in nonuniform performance. An important feature of the W/T MPR codes is that the aspect ratio can be varied by tradeoff between wavelength and temporal lengths. W/T MPR codes are superior to W/T codes [2]–[9] in terms of cardinality and spectral efficiency, for given wavelength and time dimensions. At the same time, MPR codes have the lowest values of λ_a and λ_c.

Optical orthogonal signature pattern codes (OOSPCs) need $L_T \geq N \times W \times (W-1)+1$, where $W = RW_p$ [6], and W/T MPR codes need $L_T \geq N \times W_p^2$. Let us assume it is possible to construct OOSPCs and W/T MPR codes for the minimum lengths. As seen from the earlier two relations, OOSPCs require higher temporal lengths than that of W/T MPR codes for given N and W of the codes. For convenience, instead of the actual $\{0,1\}$ notation, a W/T MPR code is represented by the chip positions of $1s$ in each row, in the order of rows from $1, 2, \cdots, R$ [10]. A W/T MPR code family of such code representations is denoted by $N(R\times W_p, L_T)$, where all the symbols have the same meanings as explained earlier. In the rest of the paper, we denote W_p as the weight/row of the W/T MPR code and as the weight of the code in OOCs. Additional modulo length (AML) codes, which are single-pulse-per-row (SPR) codes [8] when encoded in wavelength and time dimensions, are referred to as W/T SPR codes in [10], and also in this paper.

The basic design principles of the W/T MPR codes characterized by $\lambda_a = \lambda_c = 1$ is explained in detail in [10] and, for completeness, we briefly review here. The following two

Manuscript received September 28, 2006; revised March 20, 2007.

The authors are with the Department of Electrical Communication Engineering, Indian Institute of Science, Bangalore 560 012, India (e-mail: lila@ece.iisc.ernet.in; srinu@ece.iisc.ernet.in).

Digital Object Identifier 10.1109/JSTQE.2007.897673

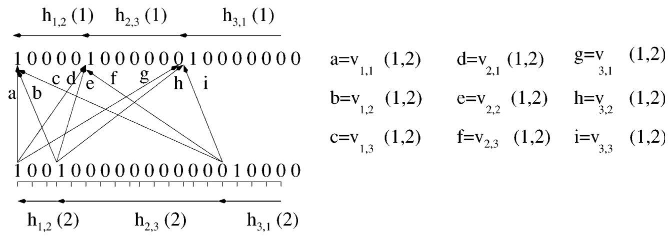

Fig. 1. Intrarow and interrow distances between 1 s in a pair of rows of a W/T MPR code.

definitions (1) and (2) are useful in calculating the intrarow and interrow distances, respectively, between 1s in a pair of rows of a W/T MPR code, which is illustrated in Fig. 1.

Let $h^a_{k,l}(i)$ denote the intrarow distance between l^{th} and k^{th} pulses in i^{th} row of a W/T MPR code a

$$h^a_{k,l}(i) = \begin{cases} l(i) - k(i), & \text{if } l(i) > k(i) \\ l(i) - k(i) + L_T, & \text{if } l(i) < k(i) \end{cases} \quad (1)$$

where $1 \le l, k \le W_p$, $l \ne k$, $1 \le i \le R$, $1 \le l(i), k(i) \le L_T$, $l(i) \ne k(i)$, $l(i)$ and $k(i)$ are the chip positions of l^{th} and k^{th} pulses, respectively, in the i^{th} row of code a.

Let $v^a_{k,l}(i,j)$ denote the interrow distance between the l^{th} pulse of j^{th} row and the k^{th} pulse of i^{th} row of a W/T MPR code a

$$v^a_{k,l}(i,j) = \begin{cases} l(j) - k(i), & \text{if } l(j) \ge k(i) \\ l(j) - k(i) + L_T, & \text{if } l(j) < k(i) \end{cases} \quad (2)$$

where $1 \le l, k \le W_p$, $1 \le i, j \le R$ and $i \ne j$, $1 \le l(j), k(i) \le L_T$, $l(j)$ and $k(i)$ are the chip positions of l^{th} and k^{th} pulses in the j^{th} and i^{th} rows, respectively, of code a.

Elements of H and V matrices are computed using (1) and (2), respectively, and the two matrices are generated for each W/T MPR code of a family. The dimensions of H and V matrices are $R \times (W_p)(W_p - 1)$ and $R(R-1)/2 \times W_p^2$, respectively. Construction of H^a and V^a matrices for a W/T MPR code a, is explained with an example for a W/T MPR code of $R = 4$ and $W_p = 3$ in (3) and (4).

Next, we state the four necessary conditions to be satisfied by a family of W/T MPR codes to have $\lambda_a = \lambda_c = 1$

$$H^a = \begin{bmatrix} h_{1,2}(1) & h_{2,3}(1) & h_{3,1}(1) & h_{1,3}(1) & \cdots \\ h_{1,2}(2) & h_{2,3}(2) & h_{3,1}(2) & h_{1,3}(2) & \cdots \\ h_{1,2}(3) & h_{2,3}(3) & h_{3,1}(3) & h_{1,3}(3) & \cdots \\ h_{1,2}(4) & h_{2,3}(4) & h_{3,1}(4) & h_{1,3}(4) & \cdots \end{bmatrix} \quad (3)$$

$$V^a = \begin{bmatrix} v_{1,1}(1,2) & v_{1,2}(1,2) & v_{1,3}(1,2) & v_{2,1}(1,2) & \cdots \\ v_{1,1}(1,3) & v_{1,2}(1,3) & v_{1,3}(1,3) & v_{2,1}(1,3) & \cdots \\ v_{1,1}(2,3) & v_{1,2}(2,3) & v_{1,3}(2,3) & v_{2,1}(2,3) & \cdots \\ v_{1,1}(1,4) & v_{1,2}(1,4) & v_{1,3}(1,4) & v_{2,1}(1,4) & \cdots \\ v_{1,1}(2,4) & v_{1,2}(2,4) & v_{1,3}(2,4) & v_{2,1}(2,4) & \cdots \\ v_{1,1}(3,4) & v_{1,2}(3,4) & v_{1,3}(3,4) & v_{2,1}(3,4) & \cdots \end{bmatrix} \quad (4)$$

A. Necessary Conditions for W/T MPR Codes

For $\lambda_a = 1$, in any W/T MPR code, a, $1 \le a \le N$, conditions (5) and (6) and for $\lambda_c = 1$, between any two W/T MPR codes a and b, $1 \le a, b \le N$, $a \ne b$, conditions (7) and (8) are necessary

$$h^a_{k,l}(i) \ne h^a_{q,r}(i), \quad \text{for } 1 \le i \le R, 1 \le k, l, q, r \le W_p, \quad k \ne l, q \text{ and } q \ne r \quad (5)$$

$$v^a_{k,l}(i,j) \ne v^a_{q,r}(i,j), \quad \text{for } 1 \le i, j \le R, i \ne j, \quad 1 \le k, l, q, r \le W_p, \text{k} \ne \text{q, and } l \ne r \quad (6)$$

$$H^a(i) \cap H^b(i) = \emptyset, \quad \text{for } 1 \le i \le R \quad (7)$$

$$V^a(i) \cap V^b(i) = \emptyset, \quad \text{for } 1 \le i \le R(R-1)/2. \quad (8)$$

The upper bound on the cardinality of W/T MPR codes for a given L_T is given by

$$N \le \left\lfloor \frac{L_T}{W_p^2} . \right\rfloor \quad (9)$$

Spectral efficiency (SE) of the W/T MPR codes is given by

$$\text{SE} = \frac{N \times \frac{1}{T_b}}{R \times \frac{1}{T_c}} = \frac{N}{R \times L_T} \quad (10)$$

where T_b is the bit time, T_c is the chip time, and $L_T = T_b/T_c$ in a code.

Optical orthogonal codes (OOCs) principle of construction, performance analysis, and construction methods are reported in [13], [14], and [15], respectively.

The organization of the paper is as follows. In Section II, we report the construction of W/T MPR codes using greedy algorithm (GA) with distinct 1-D OOCs of a family [13] as the row vectors and the representation of the results are presented. In Section III, simulation of the W/T MPR codes and matched filters, using Matlab, to verify the correlation properties of the codes, is explained and the verified results of the generated codes, using the GA, are presented. Further, we report the performance analysis of W/T MPR codes in Section IV, and also compare the cardinalities and spectral efficiencies of W/T MPR codes and multiple wavelength OOCs (MWOOCs).

II. Construction of W/T MPR Codes

In this section, we report the construction of a family of W/T MPR codes using GA with distinct 1-D OOCs of a family [13] as the row vectors. The GA algorithm is formulated to involve the four necessary conditions as different steps, starting with distinct 1-D OOCs of weight W_p as the rows of the W/T MPR codes. First, a family of OOCs of cardinality at least $\lceil \frac{N}{R} \rceil \times R$ and of weight W_p are constructed ($N \ge R$, assumed). $\lceil \frac{N}{R} \rceil$ number of W/T MPR seed codes of weight W are constructed, by using distinct sets of R OOCs. From one seed code, $(R-1)$ number of W/T MPR codes are obtained by cyclic shift of the rows of the seed code. Thus, in all, N W/T MPR codes are obtained, which satisfy conditions (5)–(7), but have to be checked for the fourth condition (8). The first condition (5) is satisfied when no distance is repeated within a row of a code, i.e., the principle of OOC, and the third condition (7) is satisfied when an OOC is not repeated in the same row, of any other W/T MPR code of a family. The second condition (6) is satisfied, when distinct

OOCs of a family form the distinct rows of a W/T MPR code, which is proved in Theorem 1 of [10]. By cyclic column shifting of the row vectors, distinct $V(i)$ distances can be obtained (for suitable L_T) for all the W/T MPR codes, whereby the fourth condition (8), is necessarily satisfied. To save memory space, code representations are used in the algorithm instead of the actual $\{0, 1\}$ code notation.

The following is the list of variables that are used in the GA:

1) $S,\ 1 \leq S \leq \lceil \frac{N}{R} \rceil$, an indicator and also the address of a W/T MPR seed code;
2) $[S]$, a W/T MPR seed code;
3) $c,\ 0 \leq c \leq R-1$, cyclic row shifts of $[S]$;
4) S_c, (all values of S and c, except 1_0, which is assumed valid), indicator of a test code; when $c = 0$, $[S_0]$ will be equal to $[S]$;
5) $A(S_c)$, address of a test code; when $c \neq 0$, $A(S_c) = \lceil \frac{N}{R} \rceil + (S-1) \times (R-1) + c$, ranges between $\lceil \frac{N}{R} \rceil + 1 \leq A(S_c) \leq N$;
6) $[A(S_c)]$, a test code;
7) $\hat{V},\ 1 \leq \hat{V} \leq N-1$, a valid code counter;
8) $R_j,\ 2 \leq j \leq R$, pointer to a row vector in $[A(S_c)]$.

The address of the code under test is obtained as follows. When $c = 0$, the address is obtained from S, otherwise, from $A(S_c)$.

A. Greedy Algorithm

1) Construct a family of OOCs of weight W_p, cardinality at least equal to $\hat{N}$=$\lceil \frac{N}{R} \rceil \times R$, and of temporal length equal to L_o [15], where L_o is the minimum temporal length needed to construct OOCs of the earlier-mentioned cardinality and weight. All the OOCs will have a "1" in the first column. Set $L_{wt} = NW_p^2$, $S = 1$, $c = 0$ and $L_T = \max\{L_o, L_{wt}\}$.
2) Construct a W/T MPR seed code $[S]$ of R rows, using R distinct OOCs as the row vectors. $[S]$ satisfies the first two conditions (5), (6). (We consider only $\lambda_a = 1$ condition for the code $[S_0] = [1_0]$ to be valid, as it is the first code.) Set $\hat{V} = 1$. Construct other W/T MPR seed codes, using R distinct sets of OOCs as the row vectors and store. Also, construct cyclic row shifts of the seed codes and store. (The seed codes and the row cyclic shifted codes satisfy the first three conditions (5)–(7). All the codes that satisfy $\lambda_a = 1$ condition, also need to satisfy $\lambda_c = 1$ between any other code in the family.)
3) Increment c. Fetch $[A(S_c)]$. (The fourth condition (8) is to be satisfied by $[A(S_c)]$ so as to qualify as another valid W/T MPR code of the family, which is described in the next step.)
4) Shift a row vector $R_j, 2 \leq j \leq R$, of the test code $[A(S_c)]$, cyclically columnwise by one, from 1 to $L_T - 1$, till $V^{S_c}(k) \cap V^q(k) = \emptyset$ for, $1 \leq k \leq j(j-1)/2$ in (4) and $1 \leq q \leq \hat{V}$.

   If this condition is not satisfied, set $L_T = L_T + 1$, $S = 1$, $c = 1$, $j = 2$, $\hat{V} = 1$ and continue from the beginning of step 4. Else, if $j < R$, increment j and continue from the beginning of step 4.

TABLE I
OOCs USED IN THE GENERATION OF W/T MPR CODES

$\hat{N}(W_p, L_o)$	OOCs				
10(2,21)	1,2	1, 3	1, 4	1,5	1,6
	1, 7	1,8	1,9	1,10	1, 11
10(3,65)	1,2,13	1,3,16	1,4,18	1,5,21	1,6,24
	1,7,26	1,8,29	1,9,31	1,10,34	1,11,37
10(4,125)	1,2,13,40	1,3,16,45	1,4,18,49	1,5,21,55	1,6,24,59
	1, 7,26,58	1,8,29,70	1,9,31,74	1,10,34,71	1,11,37,77
10(5, 232)	1,2,13,40,86	1,3,16,45,92	1,4,18,49,98	1,5,21,55,107	1,6,24,59,114
	1,7,26,58,118	1,8,29,69,133	1,9,31,68,140	1,10,34,75,137	1,11,37,80,155

TABLE II
$N(R \times W_p(=2), L_T)$ W/T MPR CODES GENERATED USING GA

10(2x2,59)									
1,2	1, 3	1, 4	1, 5	1,6	1, 7	1,8	1,9	1, 10	1, 11
1,3	6,7	11,15	14,17	21,27	24,29	32,40	36,43	46,56	49, 58
9(3x2,72)									
1,2	1,3	1,4	1,5	1,6	1,7	1,8	1,9	1,10	
1,3	11,14	7,8	17,22	28,34	21,25	31,39	44,53	35,42	
1,4	7,8	12,14	30,36	52,56	41,46	62,71	24,31	19,27	
8(4x2,97)									
1,2	1,3	1,4	1,5	1,6	1,7	1,8	1,9		
1,3	15,18	10,14	8, 9	22,28	35, 42	33,41	27,32		
1,4	8,12	22,23	13, 15	38,45	70, 78	62,67	51, 57		
1,5	32,33	9,11	18, 21	7, 15	63, 68	90,96	66, 73		

5) When (8) is satisfied by $[A(S_c)]$, increment $\hat{V}$. If $\hat{V} = N$, exit.
6) If $c < R - 1$, jump to step 3.
7) If $S < \lceil \frac{N}{R} \rceil$, increment S and fetch another seed code $[S]$. Set $c = 0$ and jump to step 4.

With $\hat{V} = N$, W/T MPR code family construction completes.

OOCs of weight 2–5 used in the generation of W/T MPR codes of $W_p = $ 2–5, respectively, are listed in Table I. Temporal length L_o in Table I indicates the length needed for the construction of $\hat{N}$ OOCs of weight W_p. W/T MPR code families $N(R \times W_p, L_T)$ of $W_p = $ 2–5 and for each value of $R = $ 2–4 are listed in Tables II–V, respectively. In the next section, we explain a method to verify the correlation properties of the constructed W/T MPR codes.

III. VERIFICATION OF THE CORRELATION PROPERTIES OF W/T MPR CODES

The autocorrelation and cross-correlation properties of the generated W/T MPR codes are verified by simulation using Matlab. The first two W/T MPR codes of $W_p = 2$ and $R = 4$ are chosen from $8(4 \times 2, 97)$ of Table II to explain the method of simulation. As the correlation of the codes is to be done in real time, we use the actual $\{0,\ 1\}$ notation of the codes, with

TABLE III
$N(R \times W_p(=3), L_T)$ W/T MPR CODES GENERATED USING GA

10(2x3,151)							
1,2,13	1,3,16	1,4,18	1,5,21	1,6,24	1,7,26	1,8,29	1,9,31
1,3,16	8,9,20	27,31,47	39,42,56	60,66,85	65,70,88	96,104,126	101,108,129
1,10,34	1, 11,37						
114,124,150	113,122,146						
9(3x3,243)							
1,2,13	1,3,16	1,4,18	1,5,21	1,6,24	1,7,26	1,8,29	1,9,31
1,3,16	29,32,46	10,11,22	38,43,61	65,71,90	58,62,78	75,83,105	109,118,142
1,4,18	10,11,22	29,31,44	67,73,92	126,130,146	101,106,124	163,172,196	213,220,241
1,10,34							
96,103,124							
24,32,54							
8(4x3,353)							
1,2,13	1,3,16	1,4,18	1,5,21	1, 6,24	1,7,26	1, 8,29	1,9,31
1,3,16	42,45,59	35,39,55	13,14,25	70,76,95	100,107,128	61,69,91	81,86,104
1,4,18	69,73,89	10,11,22	32,34,47	124,131,152	205,213,235	158,163,181	144,150,169
1,5,21	13,14,25	74,76,89	39,42,56	150,158,180	327,332,350	251,257,276	212,219,240

TABLE IV
$N(R \times W_p(=4), L_T)$ W/T MPR CODES GENERATED USING GA

10(2x4,357)					
1,2,13,40	1,3,16,45	1,4,18,49	1,5,21,55	1,6,24,59	1, 7,26,58
1,3,16,45	10,11,22,49	65,69,85,119	78,81,95,126	109,115,134,166	155,160,178,213
1,8,29,70	1,9,31,74	1 , 10, 34 , 71	1, 11, 37, 77		
197,205,227,270	204,211,232,273	249, 259, 285, 325,	284, 293, 317, 354		
9(3x4,549)					
1,2,13,40	1,3,16,45	1,4,18,49	1,5,21,55	1,6,24,59	1,7,26,58
1,3,16,45	49,52,66,97	26,27,38,65	108,113,131,166	159,165,184,216	124,128,144,178
1,4,18,49	110,111,122,149	62,64,77,106	194,200,219,251	315,319,335,369	268,273,291,326
1,8,29,70	1,9,31,74	1,10,34,71			
202,210,232,275	221,230,254,291	238,245,266,307			
30,39,63,100	446,453,474,515	472,480,502,545			
8(4x4,721)					
1,2,13,40	1,3,16,45	1,4,18,49	1,5,21,55	1,6,24,59	1,7,26,58
1,3,16,45	81,84,98,129	56,60,76,110	13,14,25,52	122,128,147,179	189,196,217,258
1,4,18,49	186,190,206,240	118,119,130,157	63,65,78,107	279,286,307,348	472,480,502,545
1,5,21,55	269,270,281,308	29,31,44,73	86,89,103,134	384,392,414,457	661,666,684,719
1,8,29,70	1,9,31,74				
205,213,235,278	165,170,188,223				
448,453,471,506	370,376,395,427				
171,177,196,228	514,521,542,583				

rows and columns representing wavelengths and time, respectively. Let $X(t)$ and $Y(t)$ be the first two W/T MPR codes of $W_p = 2$ and $R = 4$ chosen from Table II, respectively, represented as matrices of dimensions $R(=4) \times L_T(=97)$ with $\{0,\ 1\}$ entries. The elements of the first two codes determine the positions of 1s in $X(t)$ and $Y(t)$, respectively. $X(t)$ and $Y(t)$ each have four wavelength channels and the number of pulses or $1s$ per wavelength channel is equal to 2. Let $\hat{X}$ and $\hat{Y}$ be the corresponding matched filters for the codes $X(t)$ and $Y(t)$ respectively. Matrices $\hat{X}$ and $\hat{Y}$ are generated by time inverting the "1" entries of $X(t)$ and $Y(t)$, respectively. For example, the first row vector of $\hat{X}$ has 1 entries in columns $L_T - 1 = 96$, and $L_T - 2 = 95$ and the remaining entries are 0s. Since the correlation time is $2L_T - 1$ for one bit, we use the bit pattern "11" to check whether there is any overlap of the correlation signals of the adjacent bits. Let $X_1(t) = [X(t)\ X(t)]$, be the spread sequences for the bit sequence "11" using the code $X(t)$. We convolve the rows of matrix $X_1(t)$ with the corresponding rows of the matrix $\hat{X}$, and add all the results of convolved wavelength channels in time to get the autocorrelation for the code $X(t)$, for the bit pattern "11." Autocorrelation plots, Figs. 2(a)–5(a), drawn for the first two codes for $R = 4$ of Tables II–V respectively, show in-phase autocorrelation is equal to W and $\lambda_a = 1$.

Similarly, convolving the rows of the matrix $X_1(t)$ with the corresponding rows of the matrix $\hat{Y}$, and adding all the results of convolved wavelength channels in time gives the cross-correlation for the bit pattern '11'. It may be seen that $\lambda_c = 1$ in the plots of Figure 2(b) to Figure 5(b), drawn for the first two codes for $R = 4$ of Table II–V, respectively.

In the next section, we present the performance analysis of the W/T MPR codes and also compare the cardinality and spectral efficiency of the W/T MPR codes with that of MWOOCs.

IV. PERFORMANCE ANALYSIS

Various constructions of W/T codes are reported in the literature such as prime-hop, EQC-prime, W/T single-pulse-per-row (SPR), and OOSPCs. We have compared these codes with W/T MPR codes in [10] and shown that our proposed codes are superior to other codes in terms of cardinality and spectral efficiency. Another interesting W/T coding scheme, MWOOCs [16], was reported around the same time. We compare W/T MPR codes with MWOOCs in Table VI for cardinality and spectral efficiency, for given wavelength and time dimensions. For fair comparison, we have assumed the parameters 1) weight of the code W, 2) number of wavelengths λ, and 3) temporal length N_{ooc} in case of MWOOCs and L_T for W/T MPR codes, to be as close as possible and also satisfying the design criteria of the respective codes.

In MWOOCs, the time-spread OOC sequences are wavelength encoded using prime sequences. Optimal permutations or the largest cardinality of MWOOCs is obtained by using prime numbers over Galois field, with prime number p at least equal to the weight of the code [16]. MWOOCs are $M \times N$ matrices, where M is the number of rows (or available wavelengths λ), and N is the number of columns (or time slots N_{ooc}). We have assumed $M = W = p = \lambda$ for MWOOCs in Table VI. The cardinality of MWOOCs is given by $\phi_{\text{ooc}} \times p^2$, where ϕ_{ooc} is the cardinality of 1-D OOCs. The spectral efficiency, which is defined as the ratio of the number of codes to the code dimension, is equal to $\frac{\lambda^2}{(W-1)(W^2)}$ for MWOOCs.

W/T MPR codes are of dimension $R \times L_T$, where $R = W/W_p$, $W_p = 2$, and $L_T = 100$ in Table VI. From (9), it can be seen that the cardinality of MPR codes is maximum when $W_p = 1$, but by the definition of W/T MPR codes, $W_p > 1$.

TABLE V
$N(R \times W_p(=5), L_T)$ W/T MPR Codes Generated Using GA

10(2x5,726)			
1,2,13,40,86	1,3,16,45,92	1,4,18,49,98	1,5,21,55,107
1,3,16,45,92	24,25,36,63,109	132,136,152,186,238	157,160,174,205,254
1,6,24,59,114	1,7,26,58,118	1,8, 29,69,133	1,9,31,68,140
272,278,297,329,389	285,290,308,343,398	419,427,449,486,558	409,416,437,477,541
1,10,34,75,137	1,11,37,80,155		
559,569,595,638,713	584,593,617,658,720		
9(3x5,1063)			
1,2,13,40,86	1,3,16,45,92	1,4,18,49,98	1,5,21,55,107
1,3,16,45,92	73,76,90,121,170	26,27,38,65,111	153,158,176,211,266
1,4,18,49,98	26,27,38,65,111	125,127,140,169,216	333,339,358,390,450
1,6,24,59, 114	1,7,26,58,118	1,8,29,69,133	1,9,31, 68,140
225,231,250,282,342	199,203,219,253,305	346,354,376,413,485	442,451,475,516,578
541,545,561,595,647	368,373,391,426,481	698,707,731,772,834	929,936,957,997,1061
1,10,34,75,137			
396,403,424,464,528			
796,804,826,863,935			
8(4x5,1452)			
1,2,13,40,86	1,3,16,45,92	1,4,18,49,98	1,5,21,55,107
1,3,16,45,92	152,155,169,200,249	129,133,149,183,235	38,39,50,77,123
1,4,18,49,98	322,326,342,376,428	31,32,43,70,116	142,144,157,186,233
1,5,21,55,107	38,39,50,77,123	323,325,338,367,414	204,207,221,252,301
1,6,24,59,114	1,7,26,58,118	1,8,29,69,133	1,9, 31, 68, 140
277,283,302,334,394	409,416,437,477,541	375,383,405,442,514	312, 317, 335,370, 425
515,522,543,583,647	828,836,858,895,967	731,736,754,789,844	633, 639, 658, 690,750
733,741,763,800,872	1337,1342,1360,1395,1450	1205,1211,1230,1262,1322	1024,1031,1052,1092, 1156

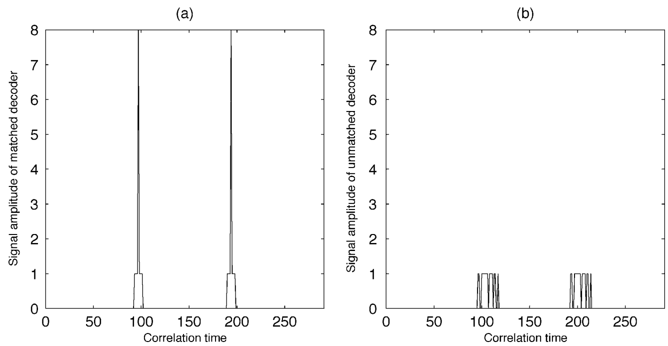

Fig. 2. (a) Autocorrelation and (b) cross-correlation of the first two W/T MPR codes of $8(4 \times 2, 97)$, for the bit pattern "11."

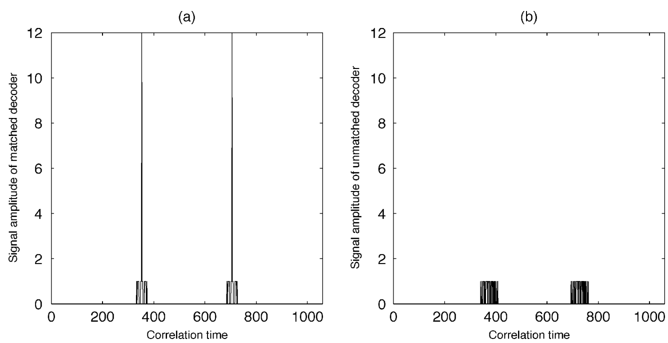

Fig. 3. (a) Autocorrelation and (b) cross-correlation of the first two W/T MPR codes of $8(4 \times 3, 353)$, for the bit pattern "11."

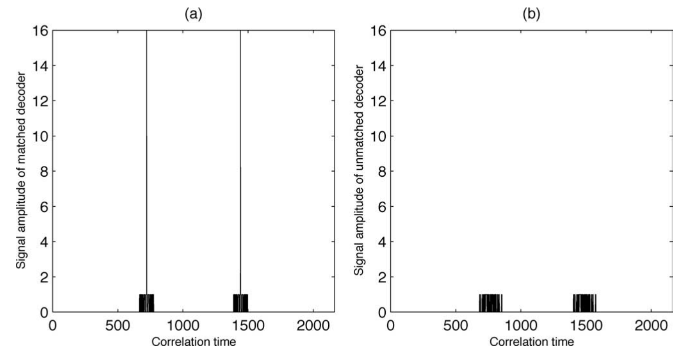

Fig. 4. (a) Autocorrelation and (b) cross-correlation of the first two W/T MPR codes of $8(4 \times 4, 721)$, for the bit pattern "11."

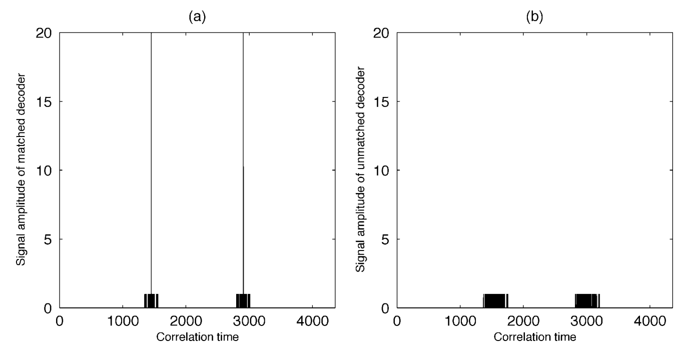

Fig. 5. (a) Autocorrelation and (b) cross-correlation of the first two W/T MPR codes of $8(4 \times 5, 1452)$, for the bit pattern "11."

Hence, we assume the next higher value $W_p = 2$, in Table VI. Also, for fair comparison, we assume $W = \lambda$ and $L_T = 100$ for W/T MPR codes. When $\lambda \geq R$, the cardinality is given by $\lfloor \frac{L_T}{W_p^2} \rfloor \times \frac{\lambda}{R}$ and the spectral efficiency of MPR codes is given by $\frac{\lambda}{W^2}$.

In Table VI, we compare MWOOCs and MPR codes for three different weights of the codes. The respective weights of the codes are chosen as close as possible after satisfying the design requirement. As we see from Table VI, W/T MPR codes achieve spectral efficiency of a given value for smaller code dimension than that of MWOOCs, whereas, for the same parameters, the cardinality is higher for MWOOCs than that of the MPR codes.

The minimum number of wavelengths needed in MWOOCs is higher than that of the W/T MPR codes, for a given set of code parameters. In MPR codes, the minimum number of wavelengths needed is equal to $R = W/W_p$, whereas, in MWOOCs, it is equal to W. In FO-CDMA networks, threshold is set equal to the weight of the code for optimum performance [10]. Another drawback of MWOOCs is that, for a given number of active users, to improve the performance, a higher Th has to be set, which can be done by increasing W and results in large increase in the temporal length, as given by (1) of [16]. Also, as the number of wavelengths required is equal to W in MWOOCs, the wavelength dimension too has to be increased. In MPR codes, however, W can be increased by increasing R (i.e., the wavelength dimension) without a large increase in the time dimension, especially when $W_p = 2$. The increase in the time dimension of the W/T MPR codes with the increase in W when $W_p = 2$ can be seen from the computed results of W/T MPR codes listed in Table II.

In an asynchronous, incoherent FO-CDMA using on-off keying, with "1" or "0" sent with equal probability, only bit "1" is encoded by the CDMA sequence. We consider a simple protocol as in [10] to analyze the performance of FO-CDMA. An ideal link is considered in which the performance deterioration is only due to the multi access interference (MAI) and the receiver noises, *i.e.*, shot noise and thermal noise are ignored. The signal at the receiver contains the desired user's signal and the interference signal I.

P_e for a W/T MPR code is given by

$$P_e = \frac{1}{2} \sum_{i=Th}^{N-1} \binom{N-1}{i} \left(\frac{RW_p^2}{2L_T} \right)^i \left(1 - \frac{RW_p^2}{2L_T} \right)^{N-1-i}. \tag{11}$$

In Fig. 6, we have analyzed the performance of MPR codes using (11) for different values of W and $L_T = 100$, when $\mathrm{Th} = W$. We have chosen $W_p = 2$ for all the curves of Fig. 6. In plotting the curves, we have assumed that the number of wavelengths available is equal to the number of rows. We see that as the weight of the code is increased, the performance improves for a given number of active users. For a given weight, the performance deteriorates with the increase in the number of active users N. When the number of interfering users is less than Th, no errors occur, only when $I \geq \mathrm{Th}$, errors occur.

TABLE VI
COMPARISON OF MWOOCS AND W/T MPR CODES FOR CARDINALITY AND SPECTRAL EFFICIENCY ($N_{\rm ooc} = L_T = 100$). $\lambda c = 1$ FOR MWOOCS AND W/T MPR CODES

Type of code	Weight (= # of wavelengths)	Code dimension	Cardinality	Spectral efficiency
MWOOC	$W = \lambda$	$W \times N_{ooc}$	$\left\lfloor \frac{N_{ooc}-1}{W(W-1)} \right\rfloor \times \lambda^2$	$\frac{\lambda^2}{(W-1)(W^2)}$
(1)	5	5×100	125	0.25
(2)	7	7×100	116	0.166
(3)	11	11×100	110	0.1
W/T MPR	$W = R \times W_p$	$R \times L_T$	$\left\lfloor \frac{L_T}{W_p^2} \right\rfloor \times \frac{\lambda}{R}$	$\frac{\lambda}{W^2}$
(1)	$4 = 2 \times 2$	2×100	50	0.25
(2)	$6 = 3 \times 2$	3×100	50	0.166
(3)	$10 = 5 \times 2$	5×100	50	0.1

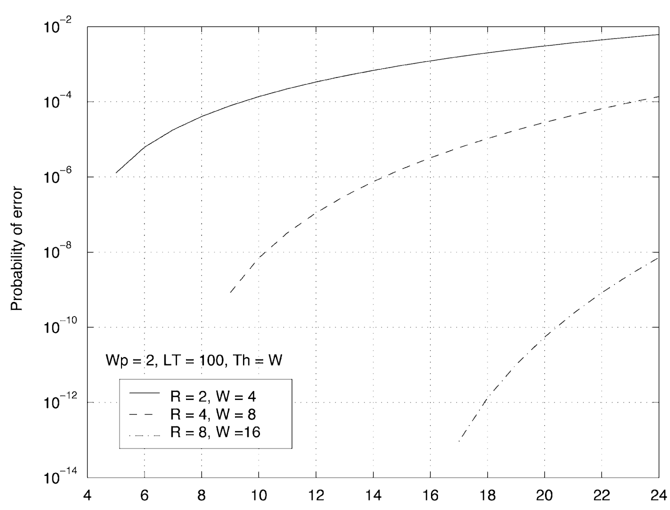

Fig. 6. Performance of the W/T MPR codes with variation in weight of the code.

V. SUMMARY

We have reported a method of construction of W/T MPR codes, for use in incoherent FO-CDMA networks, using the GA. Distinct 1-D OOCs of a family are used as the row vectors and cyclically column shifted, satisfying all the necessary conditions, so as to have minimal correlation values for W/T MPR codes. Representation of the computed results using the algorithm are presented. The correlation properties of the generated codes are verified by simulating the codes and the matched filters using the Matlab, and show that the autocorrelation peak is equal to the weight of the code and the off-peak autocorrelation and cross-correlation values are equal to one. The performance of W/T MPR codes is analyzed considering MAI as the dominant source of noise. The bit-error-rate (BER) performance of the W/T MPR codes is very good as they have minimal peak cross-correlation values equal to "1." We have shown that W/T MPR codes (having $W_p = 2$) achieve spectral efficiencies equal to that of MWOOCs, with smaller code dimensions than that of MWOOCs. Hence, it may be concluded that W/T MPR coding scheme is an ideal choice for asynchronous FO-CDMA networks.

REFERENCES

[1] J. Shah, "Optical CDMA," *Opt. Photon. News*, vol. 14, no. 4, pp. 42–47, Apr. 2003.

[2] L. Tancevski and I. Andonovic, "Wavelength hopping/time spreading code-division-multiple-access systems," *Electron. Lett.*, vol. 30, pp. 1388–1390, Aug. 1994.

[3] L. Tancevski and I. Andonovic, "Hybrid wavelength hopping/time spreading schemes for use in massive optical networks with increased security," J. Lightw. Technol., vol. 14, no. 12, pp. 2636–2647.

[4] A. I. Mendez, R. M. Gagliardi, H. X. C. Feng, J. P. Heritage, and J. M. Morookian, "Strategies for realizing O-CDMA for dense, high speed, long span, optical network applications," *J. Lightw. Technol. Special Issue on Optical Networks*, vol. 18, no. 12, pp. 1685–1696, Dec. 2000.
[5] A. J. Mendez, R. M. Gagliardi, V. J. Hernandez, C. V. Bennett, and W. J. Lennon, "Design and performance analysis of wavelength/time (W/T) matrix codes for optical CDMA," *J. Lightw. Technol.*, vol. 21, no. 11, pp. 2524–2533, Nov. 2003.
[6] G. C. Yang and W. C. Kwong, "Two-dimensional spatial signature patterns," *IEEE Trans. Commun.*, vol. 44, no. 2, pp. 184–191, Feb. 1996.
[7] F.-R. Gu and J. Wu, "Construction of two-dimensional wavelength/time optical orthogonal codes using difference family," *J. Lightw. Technol.*, vol. 23, no. 11, pp. 3642–3652, Nov. 2005.
[8] E. S. Shivaleela, K. N. Sivarajan, and A. Selvarajan, "Design of a new family of two-dimensional codes for fiber-optic CDMA networks," *J. Lightw. Technol.*, vol. 16, no. 4, pp. 501–508, Apr. 1998.
[9] R. M. H. Yim, L. R. Chen, and J. Bajcsy, "Design and performance of 2-D codes for wavelength/time O-CDMA," *IEEE Photon. Technol. Lett.*, vol. 14, no. 5, pp. 714–716, May 2002.
[10] E. S. Shivaleela, A. Selvarajan, and T. Srinivas, "Two dimensional optical orthogonal codes for fiber-optic CDMA networks," *J. Lightw. Technol.*, vol. 23, no. 2, pp. 647–654, Feb. 2005.
[11] P. K. Pepeljugoski, B. K. Whitlock, D. M. Kuchta, J. D. Crow, and S.-M. Kang, "Modeling and simulation of the OETC optical bus," in *Proc. 1995 IEEE Lasers Electro-Opt. Soc. Annu. Meeting*, vol. 1, pp. 185–186.
[12] B. K. Whitlock, P. K. Pepeljugoski, D. M. Kuchta, J. D. Crow, and S. M. Kang, "Computer modeling and simulation of the optoelectronic technology consortium (OETC) optical bus," *IEEE J. Sel. Areas Commun.*, vol. 15, no. 4, pp. 717–730, May 1997.
[13] J. A. Salehi, "Code-division-multiple-access techniques in optical fiber networks. Part I: Fundamental principles," *IEEE Trans. Commun.*, vol. 37, no. 8, pp. 824–833, Aug. 1989.
[14] J. A. Salehi and C. A. Brackett, "Code-division-multiple-access techniques in optical fiber networks. Part II: Systems and performance analysis," *IEEE Trans. Commun.*, vol. 37, no. 8, pp. 834–842, Aug. 1989.
[15] F. R. K. Chung, J. A. Salehi, and V. K. Wei, "Optical orthogonal code design analysis and application," *IEEE Trans. Inf. Theory*, vol. 35, no. 3, pp. 595–604, May 1989.
[16] W. C. Kwong, G.-C. Yang, V. Baby, C.-S. Bres, and P. R. Pruncal, "Multiple-wavelength optical orthogonal codes under prime-sequence permutations for optical CDMA," *IEEE Trans. Commun.*, vol. 53, no. 1, pp. 117–123, Jan. 2005.
[17] P. Wang and T. Le-Ngoc, "2-D optical CDMA networks using MWPM, double hard limiters and modified carrier-hopping prime sequences," *J. Lightw. Technol.*, vol. 23, no. 10, pp. 2902–2913, Oct. 2005.

E. S. Shivaleela received the M.Sc.(Eng.) degree in electrical communication engineering from the Indian Institute of Science, Bangalore, India. She is currently a Senior Scientific Officer at the Indian Institute of Science, where she is working toward the Ph.D. degree.

She is the author or coauthor of over 15 papers published in international journals in the areas of fiber-optic code-division multiple access (FO-CDMA) networks. Her current research interests include FO-CDMA, all-optical networks, and fiber and integrated optics (IO) components for photonic gigabit access systems.

T. Srinivas (S'87–M'87) received the Ph.D. degree from the Indian Institute of Science, Bangalore, India.

From 1992 to 1996, he was a Postdoctoral Fellow at Toyohashi University of Technology, Toyohashi, Japan. Currently, he is an Assistant Professor at the Department of Electrical Communication Engineering, Indian Institute of Science. He is the author or coauthor of over 50 papers published in international journals in the areas of microelectromechanical systems (MEMS), integrated optics (IO), and fiber-optic networks. His current research interests include microoptoelectromechanical systems (MOEMS), IO, fiber-optic sensors, and optical communications.